Development, Optimization and Evaluation of β-Cyclodextrin-Based Nanosponges for Solubility Enhancement of Enzalutamide

Samruddhi Sunil Mahajan*, Venkateswara Rao Javvaji
Department of Pharmaceutics, School of Pharmaceutical Sciences, Sandip University, Nashik, India
Corresponding Author: Ms. Samruddhi Sunil Mahajan, samruddhi13.99@gmail.com

ABSTRACT

Background: Enzalutamide is a potent androgen receptor inhibitor with great potency and limited aqueous solubility (approximately, 2.150 ± 0.18 0g/mL in water) since it belongs to BCS Class II. This leads to dissolution-restrained uptake and fluctuation in treatment reaction.

Methods: β-cyclodextrin nanosponges were prepared using diphenyl carbonate by the melt method at different molar ratios (1:2, 1:4, 1:6). The optimized batch (1:4) showed the highest yield (86.89%). A 3^2 factorial design was used for drug loading optimization. Preformulation studies confirmed a melting point of 199–202 °C and a linear UV calibration curve ($R^2 = 0.9918$). Characterization was performed using FTIR, DSC, SEM, particle size, and zeta potential analysis. In vitro drug release and stability studies were conducted as per ICH guidelines.

Results: The optimized nanosponge formulation showed a significant increase in solubility compared to the pure drug (~2.150 µg/mL). DSC analysis indicated reduced crystallinity, while FTIR confirmed the absence of drug–excipient interaction. The formulation exhibited high entrapment efficiency, nanoscale particle size, and uniform morphology. Dissolution studies demonstrated enhanced drug release compared to pure enzalutamide, following a non-Fickian diffusion mechanism. Stability studies under accelerated conditions (40 ± 2 °C / 75 ± 5% RH) showed no significant changes, confirming formulation stability.

Conclusion: The optimal formulation (1:4 ratio) showed better performance implying that it could be used in the management of prostate cancer by increasing oral bioavailability and therapeutic consistency.

Keywords: Enzalutamide, Nanosponges, 5 -cyclodextrin, Solubility enhancement, Factorial design, Drug delivery.

How to cite this article: Mahajan SS, Javvaji VR. Development, Optimization and Evaluation of β-Cyclodextrin-Based Nanosponges for Solubility Enhancement of Enzalutamide. Int J Drug Deliv Technol. 2026;16(16s): 573-582. DOI: 10.25258/ijddt.16.16s.61

INTRODUCTION

Cancer is a multifactorial and heterogeneous disease characterized by uncontrolled cellular proliferation, resistance to programmed cell death, sustained angiogenesis, metabolic reprogramming, and the ability to invade and metastasize [1]. It represents one of the most pressing global health challenges of the twenty-first century. Nanosponges are three-dimensional cross-linked polymeric networks characterized by nanoscale cavities and interconnected channels [2]. Their porous architecture allows entrapment of drug molecules within internal cavities and adsorption onto surface channels. Unlike conventional nanoparticles that rely solely on encapsulation, nanosponges combine inclusion complexation and matrix entrapment mechanisms [3]. The high surface area and tunable pore size contribute to enhanced drug loading capacity and improved dissolution behavior. Additionally, the cross-linked network provides mechanical stability and protects the incorporated drug from environmental degradation [4].

Cyclodextrins are cyclic oligosaccharides composed of α-(1→4)-linked glucopyranose units arranged in a toroidal structure. The outer surface is hydrophilic, while the internal cavity is relatively hydrophobic, enabling inclusion complex formation with lipophilic drugs [5]. β-Cyclodextrin is widely used due to its suitable cavity size and established safety profile [18]. However, native β-cyclodextrin has limited aqueous solubility and moderate complexation efficiency. To overcome these limitations, cross-linking β-cyclodextrin molecules produces nanosponges with enhanced structural stability and improved drug encapsulation capacity [6].

β-Cyclodextrin nanosponges are commonly synthesized using cross-linking agents such as diphenyl carbonate through the melt method [7]. In this process, hydroxyl groups of β-cyclodextrin react with diphenyl carbonate to form carbonate linkages, creating a rigid three-dimensional polymeric network [8].

MATERIAL AND METHODS

Materials: Enzalutamide was used as the drug, β-cyclodextrin as the polymer, and diphenyl carbonate as the cross-linking agent. Ethanol, distilled water, KBr, SLS, and other analytical grade reagents were used throughout the study.

Pre-formulation Studies

Determination of Melting Point: The capillary tube was placed in the melting point apparatus and heated gradually. The temperature at which the drug started melting and the temperature at which complete melting occurred were recorded. The experiment was performed in triplicate, and the average value was reported [9].

Determination of Solubility: The solubility of the drug was determined by the shake-flask method in distilled water, 0.1 N hydrochloric acid, and phosphate buffer (pH 6.8). An excess quantity of drug was added to 10 mL of each solvent in stoppered conical flasks. The flasks were placed on a mechanical shaker and agitated for 24 hours at room temperature to reach equilibrium [10].

Determination of λmax and Preparation of Calibration Curve: A standard stock solution of the drug was prepared in 0.1 N HCl. The solution was scanned in the wavelength range of 200–400 nm using a UV-Visible spectrophotometer to determine the wavelength of maximum absorbance (λmax) [11].

Drug–Excipient Compatibility Study: Drug–excipient compatibility was evaluated using FTIR and DSC analysis. A physical mixture of drug and excipients in a 1:1 ratio was prepared by triturating the components in a mortar and pestle [12].

FTIR Analysis: The physical mixture was analysed using an FTIR spectrophotometer employing the KBr pellet technique. The spectra were recorded in the range of 4000–500 cm^{-1} and compared with that of the pure drug to identify possible interactions [13].

DSC Analysis: Approximately 5 mg of the sample was sealed in an aluminium pan and analysed using a DSC instrument at a heating rate of 10 °C/min over a temperature range of 50–380 °C under nitrogen atmosphere. Thermograms of the physical mixture were compared with that of the pure drug to observe any changes in thermal behaviour [14].

Synthesis of Blank β-Cyclodextrin Nanosponges: Blank β-cyclodextrin nanosponges were prepared using the melt cross-linking method with diphenyl carbonate as the cross-linking agent. Different molar ratios of β-cyclodextrin to diphenyl carbonate (1:2, 1:4, and 1:6) were used. β-Cyclodextrin and diphenyl carbonate were accurately weighed and mixed thoroughly. The mixture was heated in a round-bottom flask at 90–100 °C under continuous stirring for 4–5 hours. During the reaction, phenol was released as a by-product, indicating cross-linking. After completion of the reaction, the mass was cooled to room temperature and pulverized. The product was subjected to Soxhlet extraction with ethanol for 24 hours to remove unreacted cross-linker and residual phenol. The purified nanosponges were dried in a hot air oven at 40 °C until constant weight was obtained and stored in a desiccator [15].

Characterization of Blank Nanosponges

Percentage Yield: The percentage yield of nanosponges was calculated to determine the efficiency of synthesis.

FTIR Analysis: FTIR spectra of β-cyclodextrin, diphenyl carbonate, and blank nanosponges were recorded to confirm cross-linking.

Differential Scanning Calorimetry: DSC analysis was performed to evaluate the thermal behavior of nanosponges and confirm the formation of a cross-linked polymeric structure.

Swelling Study: A known quantity of nanosponges was dispersed in distilled water and allowed to swell for 24 hours. The swollen nanosponges were weighed and the swelling index was calculated [16].

Drug Loading Using 3^2 Factorial Design: Drug loading was performed using a **3^2 full factorial design** to optimize formulation variables [17].

Evaluation of Drug-Loaded Nanosponges: The prepared nanosponge formulations were evaluated for the following parameters:

Entrapment Efficiency: Entrapment efficiency was determined by extracting the drug from the nanosponges and analyzing it spectrophotometrically.

Particle Size: Particle size was determined using dynamic light scattering (DLS) technique.

Saturation Solubility: The solubility of drug-loaded nanosponges was determined by the shake-flask method [18].

Statistical Analysis: The results obtained from the factorial design were fitted to a quadratic polynomial equation. Statistical analysis was performed using Design-Expert® software. Analysis of variance (ANOVA) was applied to determine the significance of model terms. Three-dimensional response surface plots and contour plots were generated to evaluate the effect of independent variables on responses [19].

RESULT AND DISCUSSION

Pre-formulation study:

Determination of Melting Point: 199-202 ℃

Determination of Solubility: Shown in table 1 and Figure 1 and 2.

Table 1. Determination of Solubility

Medium	Trial 1	Trial 2	Trial 3	Mean ± SD (µg/mL)
Water	2.123	2.343	1.983	2.150 ± 0.18
0.1 N HCl	1.945	1.678	1.765	1.796 ± 0.13
pH 6.8 Phosphate Buffer	2.234	2.231	2.341	2.269 ± 0.062

Determination of Lambda max and calibration curve:

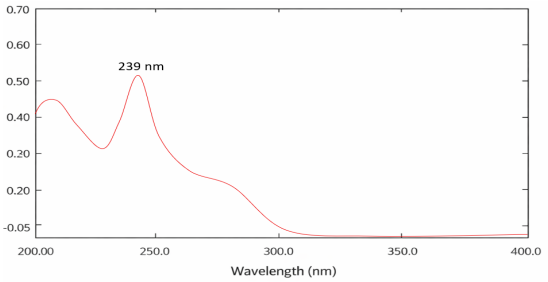

Figure 1: Determination of Absorption maxima

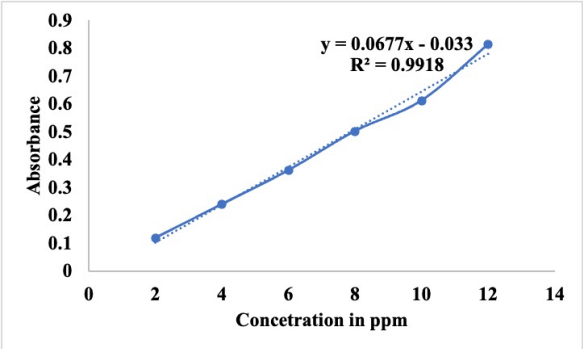

Figure 2: Calibration Curve of Enzalutamide

Drug Excipient compatibility study:

FTIR spectra of pure Enzalutamide showed characteristic functional group peaks, which were retained in physical mixtures without significant shifts or new peaks, indicating no drug–excipient interaction. DSC analysis revealed a sharp melting endotherm confirming its crystalline nature, and this peak was preserved in physical mixtures with only slight intensity changes due to dilution. Overall, both FTIR and DSC studies confirmed compatibility between Enzalutamide and the selected excipients (Figure 3).

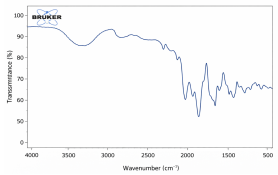

FTIR spectra of API + Beta cyclodextrin + DCP

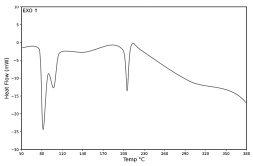

DSC of API + Excipients

Figure 3: FTIR and DSC Spectrum of API + Excipients

Characterization of Blank β-Cyclodextrin Nanosponges:

Blank nanosponges were prepared using β-Cyclodextrin and Diphenyl Carbonate in different molar ratios (1:2, 1:4 and 1:6). The preparsed batches (B1, B2 and B3) were characterized for percentage yield, FTIR, DSC and swelling index to select the optimized cross-linking ratio.

Percentage Yield:

Table 2: Percentage Yield of Blank Nanosponges

Batch Code	β-CD : DPC Ratio	Theoretical Yield (g)	Practical Yield (g)	Percentage Yield (%)
B1	1 : 2	6.89	4.75	68.94 %
B2	1 : 4	8.77	7.62	86.89 %
B3	1 : 6	10.65	8.05	75.59 %

The percentage yield of β-CD nanosponges varied with molar ratio. Batch B1 (1:2) showed moderate yield (68.94%) due to low crosslinking, while Batch B2 (1:4) exhibited the highest yield (86.89%), indicating optimal network formation. Batch B3 (1:6) showed reduced yield (75.59%) due to excessive crosslinking. Thus, the 1:4 ratio was found to be optimal for nanosponge preparation (Table 2).

FTIR Analysis of Blank β-Cyclodextrin Nanosponges:

FTIR analysis of the blank β-cyclodextrin nanosponge (1:4 ratio) showed a distinct carbonyl peak at ~1745 cm^{-1}, confirming successful cross-linking with diphenyl carbonate. A reduction in O–H stretching intensity indicated involvement of hydroxyl groups, while slight changes in the C–O–C region suggested structural modification. Absence of free cross-linker peaks confirmed effective purification and formation of a stable nanosponge network (Figure 4).

Differential Scanning Calorimetry (DSC):

The DSC thermogram of the β-cyclodextrin nanosponge (1:4 ratio) showed a broad dehydration peak around ~100 °C with reduced intensity, indicating

cross-linking. Absence of a peak for free diphenyl carbonate confirmed effective purification, while lack of a sharp melting peak suggested an amorphous structure. A broad degradation peak at 320–330 °C further confirmed formation of a stable cross-linked nanosponge network (Figure 4).

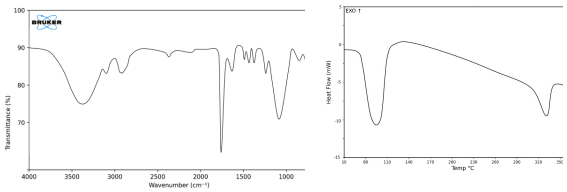

FTIR **DSC**

Figure 4: FTIR and DSC of blank nanosponges

Swelling Study:

The selected β-cyclodextrin nanosponge (1:4 ratio) showed significant swelling, indicating a porous cross-linked structure. The swelling behaviour reflects good water absorption due to hydrophilic groups while maintaining structural stability from cross-links. This balanced swelling confirms optimal crosslink density, suitable for effective drug loading and controlled release (Table 3).

Table 3: Swelling Index of Selected Blank β-CD Nanosponges (1:4)

Parameter	Observation 1	Observation 2	Observation 3	Mean ± SD
Weight of dry nanosponges (Wd) (g)	0.100	0.100	0.100	—
Weight of swollen nanosponges (Ws) (g)	0.248	0.255	0.242	—
Swelling Index (%)	148 %	155 %	142 %	148.33 ± 6.51 %

Optimization for Drug Loading:

The prepared Enzalutamide-loaded β-cyclodextrin nanosponge formulations (F1–F9) were evaluated to study the influence of formulation variables on entrapment efficiency, particle size, and saturation solubility. A 3^2 full factorial design was employed to investigate the effect of two independent variables, namely Drug: Nanosponge ratio (X_1) and ethanol volume (X_2), each at three levels. The experimental results obtained for the dependent variables are presented in Table 4.

Table 4: 3^2 Factorial Design: Drug Loading Optimization Results

Formulation Code	Drug to NS ratio (X1)	Ethanol (ml) (X2)	Entrapment Efficiency (%) (Y1)	Particle Size (nm) (Y2)	Saturation Solubility (µg/ml) (Y3)
F1	1	5	78.5	210.5	15.34
F2	1	10	82.4	215.4	16.65
F3	1	15	76.1	230.5	18.56
F4	0.5	5	84.6	213.2	19.56
F5	0.5	10	88.3	234.2	26.45
F6	0.5	15	85.8	256.4	28.45
F7	0.33	5	72.5	220.4	20.34
F8	0.33	10	71.4	260.5	25.45
F9	0.33	15	68.8	288.5	29.45

Entrapment efficiency ranged from 68.8–88.3%, with F5 showing the highest value (88.3%). Increased nanosponge proportion improved entrapment, while excessive ethanol reduced it. Particle size ranged from 210.5–288.5 nm and increased with higher ethanol volume and polymer content, though all remained nanoscale. Saturation solubility (15.34–29.45 µg/mL) significantly improved, increasing with ethanol volume and nanosponge ratio. Overall, F5 was selected as the optimized batch due to its high entrapment, acceptable particle size, and enhanced solubility.

Statistical Analysis and Model Fitting (3^2 Full Factorial Design):

The experimental data obtained from the 3^2 factorial design were analyzed using Design-Expert® software (Version 13). The effect of independent variables, Drug:Nanosponge ratio (X_1) and ethanol volume (X_2), on the dependent responses — Entrapment Efficiency (Y_1), Particle Size (Y_2), and Saturation Solubility (Y_3) — was evaluated by fitting the data to a second-order quadratic polynomial model.

Entrapment Efficiency (Y_1):

The quadratic model was found to be statistically significant ($p < 0.05$), indicating a significant influence of formulation variables on entrapment efficiency. The model F-value suggested that the model was adequate. The coefficient of determination (R^2) indicated good agreement between predicted and experimental values. Both Drug:Nanosponge ratio and ethanol volume

significantly influenced entrapment efficiency. The interaction term (X_1X_2) showed moderate effect, suggesting combined influence of both variables. The lack-of-fit was found to be non-significant ($p > 0.05$), confirming model adequacy (Table 5).

Table 5: ANOVA for Quadratic model: Entrapment Efficiency

Source	Sum of Squares	df	Mean Square	F-value	p-value	
Model	374.85	5	74.97	17.62	0.0197	significant
A-Drug to NS Ratio	98.41	1	98.41	23.13	0.0171	
B-Ethanol	3.89	1	3.89	0.9148	0.4094	
AB	0.0021	1	0.0021	0.0005	0.9836	
A²	326.24	1	326.24	76.69	0.0031	
B²	17.80	1	17.80	4.18	0.1333	
Residual	12.76	3	4.25			
Cor Total	387.61	8				

The model was significant ($F = 17.62$, $p < 0.05$), with A and A^2 as key factors influencing entrapment efficiency. The quadratic model showed that Drug: Nanosponge ratio positively affected entrapment, while ethanol volume had a slight negative effect. Significant quadratic terms indicated a nonlinear relationship, with an optimum at intermediate levels. Overall, Drug: Nanosponge ratio had the strongest influence on entrapment efficiency.

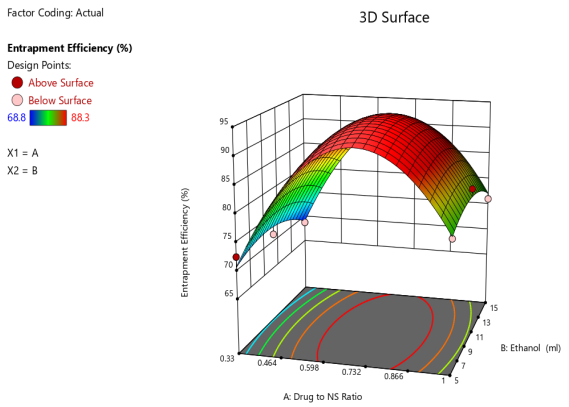

Figure 5: 3D Response Surface Plot Showing Effect of Drug: NS Ratio and Ethanol Volume on Entrapment Efficiency

The 3D response surface showed a quadratic relationship between variables and entrapment efficiency. Efficiency increased with Drug: Nanosponge ratio up to an optimum, then decreased, while ethanol volume had a moderate effect with best results at intermediate levels. The elliptical contour indicated a clear optimum region, with Drug: Nanosponge ratio having the strongest influence (Figure 5).

Particle Size (Y_2)

The quadratic model for particle size was statistically significant. Drug:Nanosponge ratio showed a considerable effect on particle size, whereas ethanol volume exhibited moderate influence. The R^2 value indicated satisfactory model predictability. The non-significant lack-of-fit further confirmed the suitability of the model (Table 6).

Table 6: ANOVA for 2FI model: **Particle Size**

Source	Sum of Squares	df	Mean Square	F-value	p-value
Model	5268.41	3	1756.14	23.60	0.0022
A-Drug to NS Ratio	1866.20	1	1866.20	25.08	0.0041
B-Ethanol	2329.07	1	2329.07	31.30	0.0025
AB	528.94	1	528.94	7.11	0.0446
Residual	372.06	5	74.41		
Cor Total	5640.48	8			

The model was significant ($F = 23.60$, $p < 0.05$), with A, B, and AB as significant factors affecting particle size. Increasing Drug:Nanosponge ratio reduced particle size, while higher ethanol volume increased it. The negative interaction term indicated a combined effect that further reduced size. The model showed a primarily linear relationship between variables and particle size.

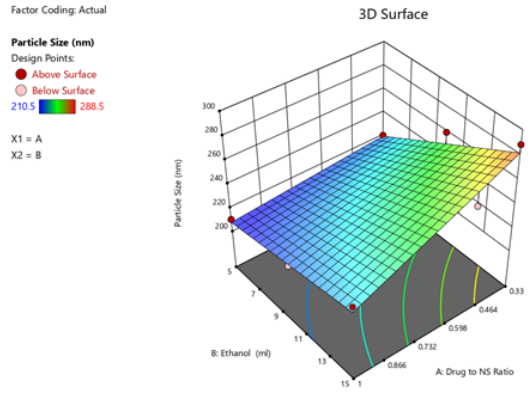

Figure 6: 3D Response Surface Plot Showing Effect of Drug: NS Ratio and Ethanol Volume on Particle Size

The 3D plot showed a mainly linear relationship between variables and particle size. Increasing Drug: Nanosponge ratio reduced size, while higher ethanol volume increased it, with a slight interaction effect. For saturation solubility, the model was significant, and both variables positively influenced solubility with a combined enhancing effect (Figure 6).

Table 7: ANOVA for Linear model: Solubility

Source	Sum of Squares	df	Mean Square	F-value	p-value
Model	200.18	2	100.09	27.82	0.0009
A-Drug to NS Ratio	125.14	1	125.14	34.79	0.0011
B-Ethanol	75.05	1	75.05	20.86	0.0038
Residual	21.58	6	3.60		
Cor Total	221.77	8			

The model was significant ($F = 27.82$, $p < 0.05$), with A and B as key factors affecting solubility. Increasing Drug: Nanosponge ratio decreased solubility, while higher ethanol volume improved it. The model showed a linear relationship with no interaction or quadratic effects (Table 7).

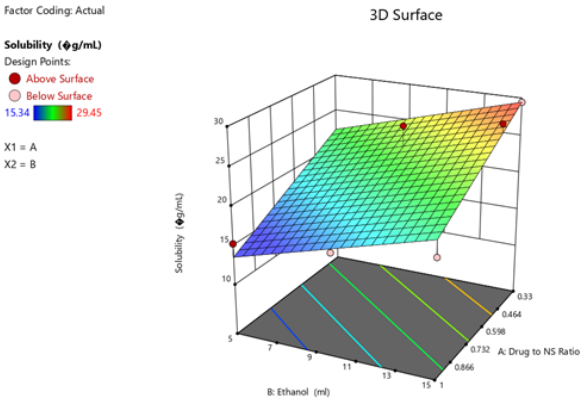

Figure 7: 3D Response Surface Plot Showing Effect of Drug: NS Ratio and Ethanol Volume on Saturation Solubility

The 3D plot showed a linear relationship for solubility. Increasing Drug:Nanosponge ratio decreased solubility, while higher ethanol volume increased it. Lack of curvature or interaction confirmed a linear model, with ethanol volume having the strongest effect. The optimized β-cyclodextrin nanosponge formulation (F5) showed a high percentage yield (84.62%), indicating efficient drug incorporation and minimal loss. Drug loading was 21.74%, confirming effective encapsulation within the nanosponge matrix. The zeta potential (–34.86 mV) indicated good colloidal stability with minimal aggregation, demonstrating suitability of the formulation for pharmaceutical use (Figure 7, Table 8).

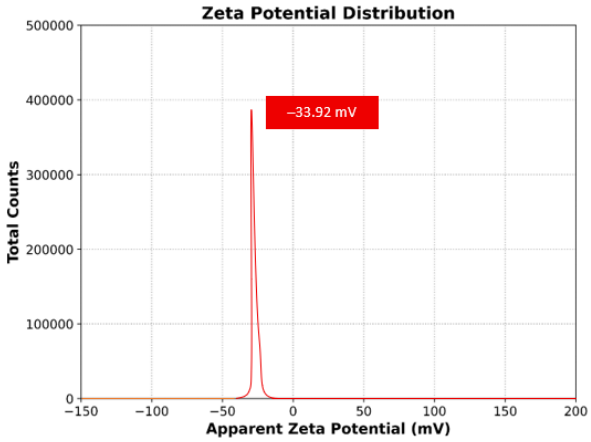

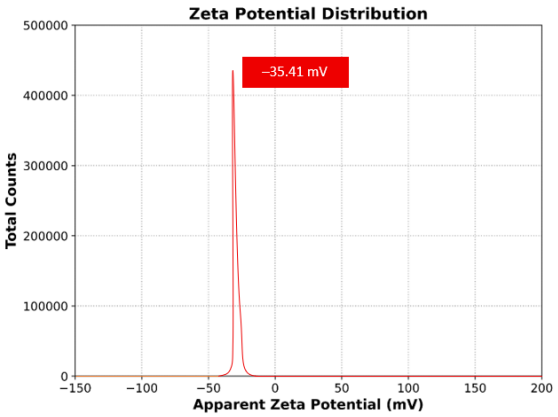

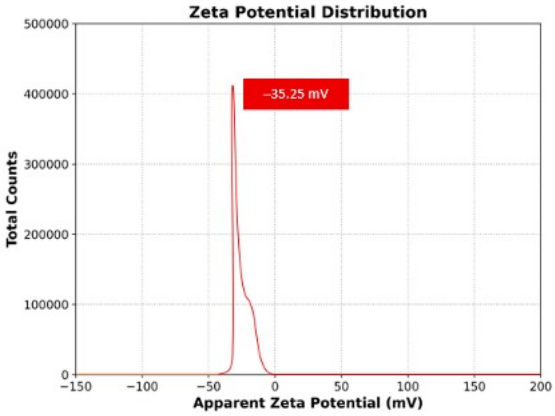

Figure 8. Zeta potential of optimised batch

Table 8: Zeta Potential of Optimized β-Cyclodextrin Nanosponge Formulation

Sr. No.	Replicate	Zeta Potential (mV)
1	R1	–33.92
2	R2	–35.41
3	R3	–35.25
	Mean ± SD	**–34.86 ± 0.82**

Scanning Electron Microscope (SEM):

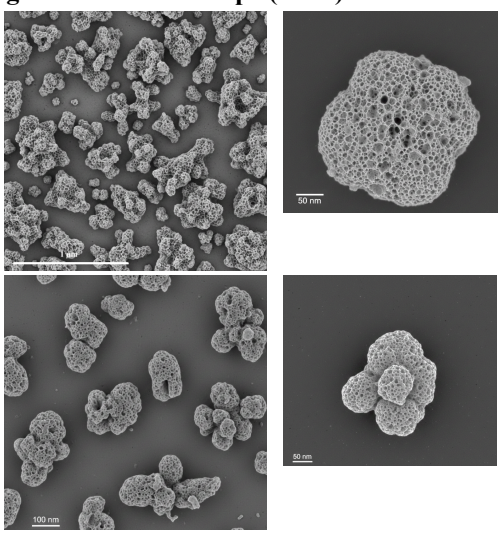

Figure 9: SEM images of optimised batch F5

SEM analysis showed irregular, porous, sponge-like nanostructures with interconnected channels, confirming successful cross-linking. The highly porous morphology supports efficient drug encapsulation and controlled release, with no visible crystalline drug on the surface indicating effective drug incorporation.

In Vitro Drug Release Study:

The optimized nanosponge formulation showed significantly improved drug release (92.5% in 12 hours) compared to pure Enzalutamide (55.4%). Enhanced dissolution was due to increased surface area, porous structure, improved wettability, and uniform drug dispersion, with no burst release observed (Table 9, Figure 10).

Table 9: Comparative In Vitro Drug Release Profile

Time (hr)	% Drug Release (Pure Drug)	% Drug Release (Optimized F5 batch)
0	0 ± 0.00	0 ± 0.00
0.5	8.4 ± 0.52	14.6 ± 0.74
1	14.6 ± 0.68	27.4 ± 1.12
2	22.8 ± 0.95	43.7 ± 1.35
3	28.5 ± 1.10	54.5 ± 1.42
4	34.2 ± 1.26	69.3 ± 1.58
6	41.8 ± 1.34	82.6 ± 1.66
8	47.3 ± 1.48	88.9 ± 1.52
10	51.6 ± 1.36	91.4 ± 1.40
12	55.4 ± 1.52	92.5 ± 1.28

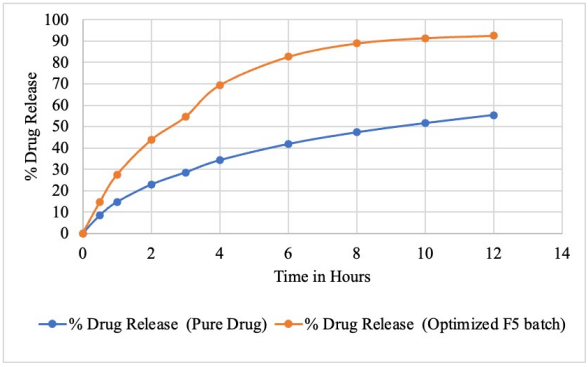

Figure 10: Graph showing % of dissolution of Pure drug versus % drug release from optimised F5 batch.

Drug Release Kinetics:

The release data best fit the First order model (R^2 = 0.9719), indicating concentration-dependent release. The Higuchi model also showed high correlation, confirming diffusion involvement. The Peppas exponent (n = 0.5808) indicated non-Fickian diffusion, suggesting a combined mechanism of diffusion and matrix relaxation (Figure 11).

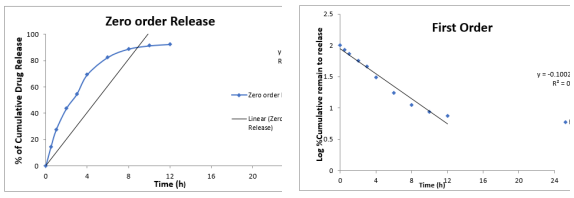

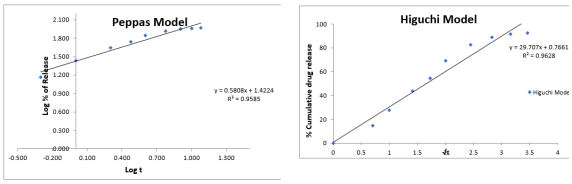

Figure 11: Drug Release Kinetic Model Plots of Optimized F5 β-Cyclodextrin Nanosponge Formulation

Stability Study:

The stability study of the optimized Enzalutamide-loaded β-cyclodextrin nanosponge formulation was conducted under accelerated storage conditions (40 ± 2 °C / 75 ± 5% RH) for a period of three months. The formulation was evaluated at 0, 1, 2, and 3 months for physical appearance, entrapment efficiency, particle size, saturation solubility, and in vitro drug release (Table 10).

Table 10: Stability Study Data of Optimized F5 Formulation Under Accelerated Conditions

Time (Month)	Appearance	Entrapment Efficiency (%)	Particle Size (nm)	Saturation Solubility (µg/mL)	% Drug Release (12 hr)
0	Off-white powder	88.3 ± 1.2	234.2 ± 5.4	26.45 ± 1.2	92.5 ± 1.3
1	No change	87.6 ± 1.4	238.6 ± 6.1	26.10 ± 1.4	91.8 ± 1.5
2	No change	87.2 ± 1.5	241.3 ± 6.8	25.82 ± 1.5	91.2 ± 1.7
3	No change	86.9 ± 1.6	244.8 ± 7.3	25.40 ± 1.6	90.6 ± 1.8

The stability data of the optimized F5 formulation under accelerated conditions are presented in Table X. No significant variation was observed in the evaluated parameters over the three-month study period.

DISCUSSION:

The present study was designed to enhance the solubility and dissolution behavior of Enzalutamide by developing β-cyclodextrin-based nanosponges using diphenyl carbonate as a cross-linking agent and optimizing the formulation through a 3^2 full factorial design. The melting point of Enzalutamide (199–202 °C) confirmed its purity and agreement with reported values. Solubility studies revealed extremely low aqueous solubility (~2 µg/mL), justifying the need for formulation strategies to improve its dissolution. The calibration curve exhibited good linearity, validating the analytical method. FT-IR and DSC analysis of the pure drug confirmed its crystalline nature, indicated by a sharp melting endotherm and characteristic functional group peaks. Compatibility studies of physical mixtures showed no significant changes in these peaks, confirming the absence of drug–excipient interaction and suitability of β-cyclodextrin and diphenyl carbonate. Among the tested molar ratios (1:2, 1:4, 1:6), the 1:4 ratio showed the highest yield (86.89%), indicating optimal crosslinking. FTIR and DSC of blank nanosponges confirmed successful formation of a stable amorphous network. The swelling index (148.33%) suggested a balanced porous structure suitable for drug loading. Factorial design results showed that drug:nanosponge ratio significantly influenced entrapment efficiency (68.8–88.3%), while ethanol volume affected particle size (210–288 nm) and solubility. Saturation solubility increased significantly (15.34–29.45 µg/mL), representing nearly 10–14 fold enhancement. The optimized formulation (F5) showed high yield, good drug loading (21.74%), and excellent stability (–34.86 mV). SEM confirmed a porous morphology. The optimized formulation exhibited enhanced drug release (92.5% in 12 hours) compared to pure drug (55.4%). Release followed first-order kinetics with non-Fickian diffusion. Stability studies indicated no significant changes, confirming robustness of the formulation.

CONCLUSION

The present study focused on the development and optimization of Enzalutamide-loaded β-cyclodextrin nanosponges using diphenyl carbonate as a cross-linking agent to enhance the solubility and dissolution of the poorly water-soluble drug. Preformulation studies confirmed its low aqueous solubility and crystalline nature, supporting the need for solubility enhancement. Compatibility studies using FTIR and DSC showed no chemical interaction between drug and excipients. Nanosponges were successfully prepared by the melt cross-linking method, with the 1:4 (β-CD:DPC) ratio showing optimal yield, structure, and swelling behavior. Characterization confirmed the formation of a stable amorphous nanosponge network. A 3^2 factorial design was applied for optimization. Drug:nanosponge ratio and ethanol volume significantly affected entrapment efficiency, particle size, and solubility. The optimized formulation (F5) showed high entrapment efficiency, nanoscale size, improved solubility, and good stability (–34.86 mV).

SEM analysis revealed porous structures suitable for drug loading. The formulation exhibited enhanced drug release (92.5% in 12 hours) compared to pure drug (55.4%). Drug release followed first-order kinetics with a non-Fickian mechanism. Stability studies confirmed no significant changes, indicating formulation stability.

DECLARATIONS:

Ethics approval and consent to participate:

Not applicable.

Consent for publication:

All the authors approved the manuscript for publication.

Availability of data and material:

All required data is available.

Competing interests:

All authors declare no competing interests.

Funding:

Not applicable.

REFERENCES:

1. Sung H, Ferlay J, Siegel RL, Laversanne M, Soerjomataram I, Jemal A, et al. Global cancer statistics 2020: GLOBOCAN estimates of incidence and mortality worldwide for 36 cancers in 185 countries. *CA Cancer J Clin.* 2021;71(3):209-249. DOI: 10.3322/caac.21660
2. Siegel RL, Miller KD, Wagle NS, Jemal A. Cancer statistics, 2023. *CA Cancer J Clin.* 2023;73(1):17-48. DOI: 10.3322/caac.21763
3. Litwin MS, Tan HJ. The diagnosis and treatment of prostate cancer: A review. *JAMA.* 2017;317(24):2532-2542. DOI: 10.1001/jama.2017.7248
4. Lonergan PE, Tindall DJ. Androgen receptor signaling in prostate cancer development and progression. *J Carcinog.* 2011;10:20. DOI: 10.4103/1477-3163.83937
5. Watson PA, Arora VK, Sawyers CL. Emerging mechanisms of resistance to androgen receptor inhibitors in prostate cancer. *Nat Rev Cancer.* 2015;15(12):701-711. DOI: 10.1038/nrc4016
6. Feldman BJ, Feldman D. The development of androgen-independent prostate cancer. *Nat Rev Cancer.* 2001;1(1):34-45. DOI: 10.1038/35094009
7. Tran C, Ouk S, Clegg NJ, Chen Y, Watson PA, Arora V, et al. Development of a second-generation antiandrogen for treatment of advanced prostate cancer. *Science.* 2009;324(5928):787-790. DOI: 10.1126/science.1168175
8. Scher HI, Fizazi K, Saad F, Taplin ME, Sternberg CN, Miller K, et al. Increased survival with enzalutamide in prostate cancer after chemotherapy. *N Engl J Med.* 2012;367(13):1187-1197. DOI: 10.1056/NEJMoa1207506
9. Beer TM, Armstrong AJ, Rathkopf DE, Loriot Y, Sternberg CN, Higano CS, et al. Enzalutamide in metastatic prostate cancer before chemotherapy. *N Engl J Med.* 2014;371(5):424-433. DOI: 10.1056/NEJMoa1405095
10. Fizazi K, Scher HI, Molina A, Logothetis CJ, Chi KN, Jones RJ, et al. Abiraterone acetate for treatment of metastatic castration-resistant prostate cancer: Final overall survival analysis. *Lancet Oncol.* 2014;15(11):1147-1156. DOI: 10.1016/S1470-2045(14)70379-0
11. Amidon GL, Lennernäs H, Shah VP, Crison JR. A theoretical basis for a biopharmaceutic drug classification. *Pharm Res.* 1995;12(3):413-420. DOI: 10.1023/A:1016212804288
12. Gibbons JA, Ouatas T, Krauwinkel W, Ohtsu Y, van der Walt JS, Beddo V, et al. Clinical pharmacokinetic studies of enzalutamide. *Clin Pharmacokinet.* 2015;54(10):1043-1055. DOI: 10.1007/s40262-015-0271-5
13. Savjani KT, Gajjar AK, Savjani JK. Drug solubility: Importance and enhancement techniques. *ISRN Pharm.* 2012;2012:195727. DOI: 10.5402/2012/195727
14. Noyes AA, Whitney WR. The rate of solution of solid substances in their own solutions. *J Am Chem Soc.* 1897;19:930-934. DOI: 10.1021/ja02086a003
15. Zhang L, Wu F, Lee SC, Zhao H, Zhang L. pH-dependent drug-drug interactions for weak base drugs. *Clin Pharmacol Ther.* 2008;83(5):761-769. DOI: 10.1038/sj.clpt.6100407
16. Trotta F, Dianzani C, Caldera F, Mognetti B, Cavalli R. Cyclodextrin nanosponges for cancer drug delivery. *Int J Pharm.* 2010;388(1-2):146-153. DOI: 10.1016/j.ijpharm.2009.12.056

17. Loftsson T, Duchêne D. Cyclodextrins and their pharmaceutical applications. *Int J Pharm.* 2007;329(1-2):1-11. DOI: 10.1016/j.ijpharm.2006.10.044
18. Trotta F, Tumiatti V, Cavalli R, Roggero C, Mognetti B, Berta GN. Cyclodextrin-based nanosponges as drug carriers. *J Incl Phenom Macrocycl Chem.* 2006;56:197-203. DOI: 10.1007/s10847-006-9086-5
19. Selvamuthukumar S, Anandam S, Kannan K, Manavalan R. Nanosponges: A novel drug delivery system. *J Pharm Pharm Sci.* 2012;15(1):103-111. DOI: 10.18433/J3C30M